Several Control Strategies for Parallel Connected Dual Induction Engines by means of a Digital-Based System Control

R. Peña-Eguiluz,[1,2] M. Pietrzak-David,[2] B. de Fornel [2]

[1] Instituto Nacional de Investigaciones Nucleares, Laboratorio de Física de Plasmas
AP 18-1027, 11801 México D. F., México
[2] Laboratoire d'Electrotechnique et d'Electronique Industrielle
Unité Mixte de Recherche INPT-ENSEEIHT / CNRS N° 5828
B.P. 7122 - 2 rue Camichel - 31071 Toulouse Cedex 7 - Toulouse, France
rpe@nuclear.inin.mx

Abstract. This paper deals with the description, implementation and simulation of four different digital control circuits proposed for a single voltage-source inverter (mono-inverter) supplying two parallel connected induction (dual induction) engine systems. Several loses in the degrees of freedom result from the connection of two motors in parallel. Therefore, four non-conventional DSP-FPGA based control strategies are proposed in this paper in order to compensate for the restrictions imposed by the high-power structure. A brief description of the proposed high-power system model, representing a commercial locomotive and its associated digital-control structure is presented. The principles of four control methodologies are discussed and analyzed. With an aim to demonstrate the resulting system operation, one mechanical perturbation has been applied to it, namely the loss of adherence of a wheel to its rail. The four system responses are assessed by simulation and compared among themselves, establishing the principal differences between the four proposed digital control methods.

1 Introduction

The multi-converter multi-machine systems (MMS) are used in several industrial applications. One of these systems may be implemented by a mono-inverter dual induction machine working with a common mechanical load [1, 2]. The structure goal consists in the quantity and size reduction of the required power electronics and control system components, decreasing the maintenance cost and by the way the price of construction [3]. This kind of structure can be applied in several industrial areas like electrical propulsion systems that have components on board, such as the robots, bus, ship, electrical and hybrid vehicles. It can be extended and applied on speed or positional control of usually conveyors.

In this paper a simulation model with a particular configuration is represented by a mid-bogie of a railway traction locomotive. It is powered by two similar asynchronous motors, which are supplied by a single voltage-source inverter (VSI). A DSP-FPGA based system is used as a digital unit control. A DSP processes the measured engines signals (currents and mechanical speeds) in order to capture the appropriated

© A. Gelbukh, H. Calvo (Eds.)
Titulo del Libro
Research on Computing Science 13, 2005, pp. 227-239

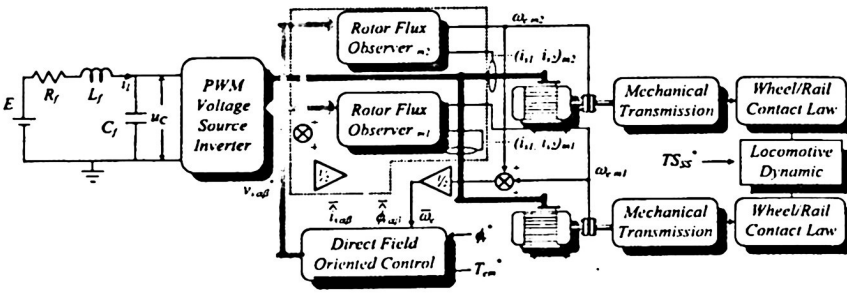

Fig. 1. The high power system working with a dual rotor flux observer structure.

semiconductor firing signal sequence from a modified Field Oriented Control (FOC) working with an innovative rotor flux full-order observer structure. Meanwhile, a FPGA produces the firing pulses to the semiconductors of the VSI at an appropriated frequency rate, which is always higher than the voltage frequency applied to the engines, provided that a Pulse Width Modulation (PWM) technique is applied to control the VSI. This kind of system is feasible if and only if an adequate control maintains an equal electromagnetic torque on the two engines even if their speeds differ.

2 System description

The model representation of the high-power system that has been studied is shown in Fig. 1. It is mainly composed by two similar squirrel cage induction engines, supplied by a PWM controlled VSI. A DC voltage source (E) is connected to the inverter through a passive (R_f, L_f, and C_f) input filter. A digital control unit made from a DSP-FPGA association takes care of the rotor flux observation, the electrical rotor speed measurement, the control algorithm and the semiconductors commutation signal generation. Each engine drives an identical mechanical transmission line, which provides the traction force transmitted to the wheels. A wheel-rail non-linear contact law, defines this traction force [4]. The locomotive dynamics is common to both engines, so that they are linked mechanically. A singular characteristic is established in this kind of structure because both engines are electrically and mechanically linked by the VSI, reducing the control degrees of freedom, and by the mechanical load, respectively. The FOC high performance function is made possible when appropriated electromagnetic engine information is provided to it. Thus, in order to control properly the high-power system, several FOC algorithm adaptations have to be carried out.

3 Rotor Flux Estimation

Many industrial high-performance engine applications depend on the adequate knowledge of the internal engine state. Taking into account the excessive cost in-

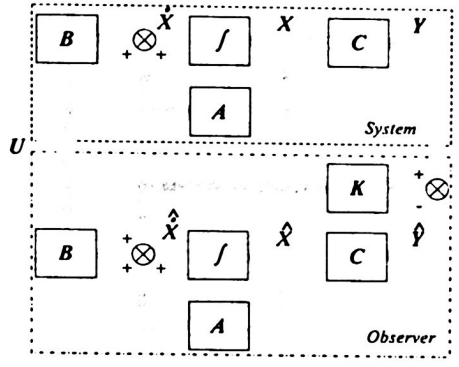

Fig. 2 General deterministic observer structure.

crease that normally occurs when a flux detector is incorporated to the engine, the use of an indirect flux detection, *e.g.* the rotor flux full-order deterministic Luenberger observer, is often desirable. Its general structure is shown in Fig. 2.

This kind of observer estimates the stator current and the rotor flux components simultaneously. It can be determined in a stationary reference frame by the next equation:

$$\dot{\hat{X}} = (A - KC)\hat{X} + BU + KCX \tag{1}$$

where:

$$X = \begin{bmatrix} i_{s\alpha} \\ i_{s\beta} \\ \phi_{r\alpha} \\ \phi_{r\beta} \end{bmatrix}, \quad A = \begin{bmatrix} a_1 & 0 & a_2 & a_3\omega_e \\ 0 & a_1 & -a_3\omega_e & a_2 \\ a_4 & 0 & a_5 & -\omega_e \\ 0 & a_4 & \omega_e & a_5 \end{bmatrix}, \quad K = \begin{bmatrix} k_1 & -k_2 \\ k_2 & k_1 \\ k_3 & -k_4 \\ k_4 & k_3 \end{bmatrix},$$

$$C = \begin{bmatrix} 1 & 0 & 0 & 0 \\ 0 & 1 & 0 & 0 \end{bmatrix}, \quad B = \begin{bmatrix} \dfrac{1}{\sigma L_s} & 0 & 0 & 0 \\ 0 & \dfrac{1}{\sigma L_s} & 0 & 0 \end{bmatrix}^T, \quad U = \begin{bmatrix} v_{s\alpha} \\ v_{s\beta} \end{bmatrix},$$

$$a_1 = \left(\frac{1}{\sigma\tau_s} + \frac{1-\sigma}{\sigma\tau_r} \right), \; a_2 = \frac{1-\sigma}{\sigma\tau_r L_m}, \; a_3 = \frac{1-\sigma}{\sigma L_m}, \; a_4 = \frac{L_m}{\tau_r}, \; a_5 = -\frac{1}{\tau_r}.$$

The observer's gain matrix, which is operated as *A-KC*, determines the observer convergence dynamics. Values of the gain matrix *K* have been calculated by applying a novel approach. It consists in establishing the observer response or 'observer root-locus' (*ORL*) to be proportional to the 'induction engine root-locus' (*IMRL*). This adaptable observer is defined by the calculated flux observer gain matrix values defined by

$$
\begin{aligned}
k_1 &= d \\
k_2 &= (1-k)\omega_e \\
k_3 &= \frac{b_1}{a_3} + \frac{a_2(b_2 - a_2 b_1)}{a_3 a_2^{\,2} + a_3^{\,3}\omega_e^{\,2}} \\
k_4 &= \frac{\omega_e(b_2 - a_2 b_1)}{a_2^{\,2} + (a_3\,\omega_e)^2}
\end{aligned}
\tag{2}
$$

where:

$$
b_1 = d\left(\frac{k}{2} - 1\right) + (1-k)(a_1 + a_3 a_4 - a_5),
$$

$$
b_2 = a_3\left[\frac{d}{2}\left(\frac{d}{2} - a_1 + a_5\right) + (k-1)\omega_e^{\,2}\right].
$$

So, the observer dynamics mainly depends on the electric engine speed, on several engine parameters and on two adjusting coefficients. The displacement coefficient d can be adjusted by increasing or reducing the observer time response. This becomes faster than the system time response as d is smaller than the unity. It means that the *ORL* origin can be shifted, from the *IMRL* origin, $d/2$ real units towards the original complex plane or towards the negative complex plane, reducing the observer time response. The damping coefficient k can be altered in order to increase or reduce the real component of the dominant complex poles. The observer damping factor can be increased if k is smaller than the unity. As a result, the system performance will be improved reducing the oscillation effects of the engine response.

It can be seen from Fig. 3 that the *ORL* has a slower time response than the *IMRL*, because it is placed ten units toward the negative complex plane. Furthermore, the *ORL* has a better damping factor then the *IMRL*, because its complex values have lower angles with respect to the real axis. Both root-locus responses have been calculated as a function of the electrical rotation speed ω_F, which has been varied from 0 to 100 rad/s. Meanwhile, the *ORL* was obtained considering the same range of ω_F, and imposing the coefficients $k = 0.5$ and $d = 20$. In order to increase the time response of the implemented system, it is necessary to apply a d coefficient lower than the unity, so that it was chosen to be 0.9. Meanwhile, the other coefficient, k, was assumed equal to the unity. Consequentially, the response of the observer became accelerated in relation to the engine response, without any damping modification.

4 Dual Motor Drive Control Structures

The novel dual engine drive control configurations presented in this paper are based on the classical FOC method, although several FOC adaptations must be imposed on each one of these structures. As every specific system regulation produces several differences on the system behavior, the system under operation could be altered in different ways when a perturbation arrives. The four different studied control methods are briefly described as follows:

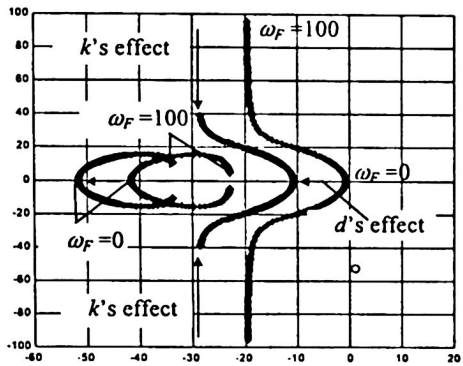

Fig. 3. Induction motor and observed root-locus as a function of the reference frame frequency.

4.1 Mean Drive Control

The mean drive control structure, shown in Fig. 1, takes into consideration the necessary signals of both engines in order to recreate an "imaginary mean engine" with the "average engine variables". It has implemented using the "dual rotor flux observer" as it provides the most adequate flux estimate [5]. The observed variable space state vector and the electrical rotor speed used in this structure are defined respectively by:

$$\mathbf{X} = \left[\frac{\hat{i}_{s\alpha\_m1} + \hat{i}_{s\alpha\_m2}}{2} \quad \frac{\hat{i}_{s\beta\_m1} + \hat{i}_{s\beta\_m2}}{2} \quad \frac{\hat{\phi}_{r\alpha\_m1} + \hat{\phi}_{r\alpha\_m2}}{2} \quad \frac{\hat{\phi}_{r\beta\_m1} + \hat{\phi}_{r\beta\_m2}}{2} \right]^T \tag{3}$$

$$\omega_e = \frac{\omega_{e\_m1} + \omega_{e\_m2}}{2} \tag{4}$$

The improved FOC as a function dependent on the engine variables takes the form:

$$FOC1(\hat{i}_{s\alpha}, \hat{i}_{s\beta}, \hat{\phi}_{r\alpha}, \hat{\phi}_{r\beta}, \omega_e) = (v_{s\alpha}{}^*, v_{s\beta}{}^*) \tag{5}$$

4.2 Switched Master – Slave Drive Control

The implemented FOC adaptation alternates the necessary inputs from the two estimated and measured engine signals every sampling time period (T_S). This is done using a multiplexed function, which provides the state signals of one engine, every sampling time period. The state variables of the engine considered, usually called "master engine", are adjusted by the control. Meanwhile, the other one, called "slave engine", is not considered until the next sampling time period $(k_T + 1)T_S$. Therefore, in the point of view of each engine, the T_S used by the FOC is twice as long as in the previ-

ous control method. Even if the FOC algorithm uses the output of only one rotor flux observer each T_S, the two observers must work continuously. This drive control configuration is shown in Fig. 4. In this case, the function which defines the drive control method becomes:

$$FOC2(\hat{i}_{s\alpha\_mi}, \hat{i}_{s\beta\_mi}, \hat{\phi}_{r\alpha\_mi}, \hat{\phi}_{r\beta\_mi}, \omega_{e\_mi}) = (v_{s\alpha}{}^*, v_{s\beta}{}^*) \tag{6}$$

$$mi = \begin{cases} m1 \text{ if } k_T = \text{odd}, \\ m2 \text{ if } k_T = \text{even}. \end{cases}$$

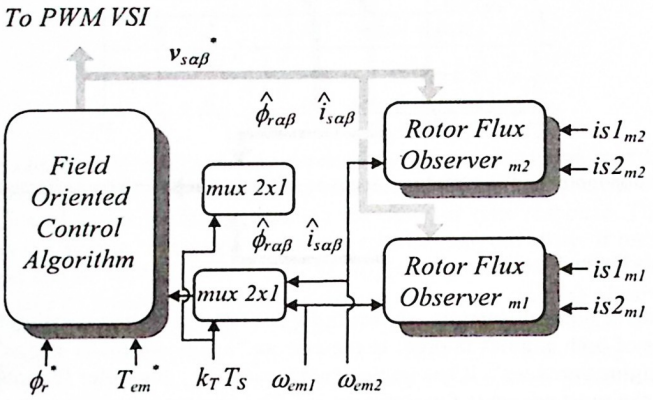

Fig. 4. The Switched Master-Slave drive control structure simplified bloc representation.

4.3 Mean Drive Control for Dual Motor

In this case the induction engines are adjusted by the regulation functions of the classical FOC in the same sampling time period, as it can be seen in Fig. 5. The VSI reference signals obtained at the end of the two regulation processes are averaged, producing the new stator voltage references. A speed engine detector and a rotor flux estimator are essential for the drive control operation of both engines. Yet, the processing time of the resulting algorithm is extended given the necessary in-line computation of two regulation processes. This control method can be represented by the equation:

$$FOC3(FOC_{m1}, FOC_{m2}) = \left(\frac{v_{s\alpha\_m1}{}^* + v_{s\alpha\_m2}{}^*}{2}, \frac{v_{s\beta\_m1}{}^* + v_{s\beta\_m2}{}^*}{2} \right) = \left(v_{s\alpha}{}^*, v_{s\beta}{}^* \right) \tag{7}$$

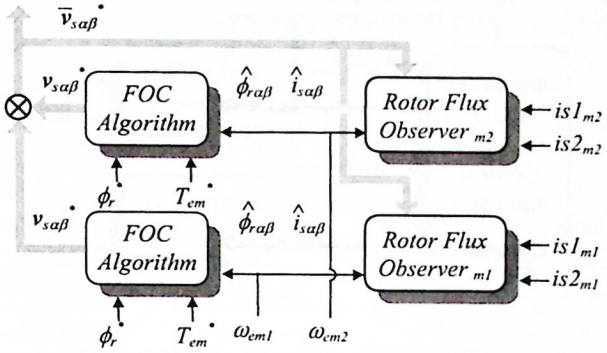

Fig. 5. The Dual Motor Mean Drive control structure simplified bloc representation.

4.4 Mean and Differential Drive Control of Dual Motor

A mean and differential drive control of dual engines has been proposed in [3]. As shown in Fig. 6, it is capable of controlling two different variables by one of the two FOC regulation axes. This is accomplished by the *d* axis regulation which takes care of the differential engine torque regulation besides that of the rotor flux, as it is the case of the classical FOC. A special transition function between these two is needed for an appropriated system operation.

Equations (8) and (9) define respectively two functions relating the electromagnetic torque and the differential electromagnetic torque produced by the dual engine system. From these equations, it is possible to obtain the expressions of regulation that have been implanted in the dual engine FOC algorithm.

$$\overline{T} = \frac{\overline{T}_{em} - \Delta T_{em}\,\Delta L_T / \overline{L}_T}{1 - \left(\Delta L_T / \overline{L}_T\right)^2} = P\,\overline{L}_T\left(\bar{\boldsymbol{i}}_{mr} \times \bar{\boldsymbol{i}}_s + \Delta \boldsymbol{i}_{mr} \times \Delta \boldsymbol{i}_s\right) \tag{8}$$

$$\Delta T = \frac{\Delta T_{em} - \overline{T}_{em}\,\Delta L_T / \overline{L}_T}{1 - \left(\Delta L_T / \overline{L}_T\right)^2} = P\,\overline{L}_T\left(\bar{\boldsymbol{i}}_{mr} \times \Delta \boldsymbol{i}_s + \Delta \boldsymbol{i}_{mr} \times \bar{\boldsymbol{i}}_s\right) \tag{9}$$

where:

$$\overline{L}_T = \frac{1}{2}\left(\frac{L_{m\_m2}^{\ 2}}{\tau_{r\_m2}} + \frac{L_{m\_m1}^{\ 2}}{\tau_{r\_m1}}\right), \quad \Delta L_T = \frac{1}{2}\left(\frac{L_{m\_m2}^{\ 2}}{\tau_{r\_m2}} - \frac{L_{m\_m1}^{\ 2}}{\tau_{r\_m1}}\right).$$

Meanwhile the control structure can be defined from the expression

$$FOC4(\hat{i}_{s\alpha\_m1}, \hat{i}_{s\beta\_m1}, \hat{\phi}_{r\alpha\_m1}, \hat{\phi}_{r\beta\_m1}, \omega_{e\_m1}, \hat{i}_{s\alpha\_m2}, \hat{i}_{s\beta\_m2}, \hat{\phi}_{r\alpha\_m2}, \hat{\phi}_{r\beta\_m2}, \omega_{e\_m2}) = (v_{s\alpha}{}^*, v_{s\beta}{}^*) \tag{10}$$

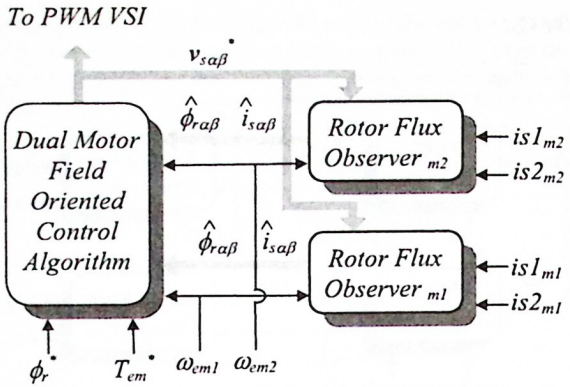

Fig. 6. The Mean and Differential Drive Control for Dual Motor Structure simplified bloc.

The hardware considered for the implementation of the proposed digital-control structures is composed by a DSP-FPGA card, named as PEC-31. It is supported by a measurement card, a protection interface, a distribution rack and a high power bloc. These elements and its interconnectivity are show in the Fig. 7.

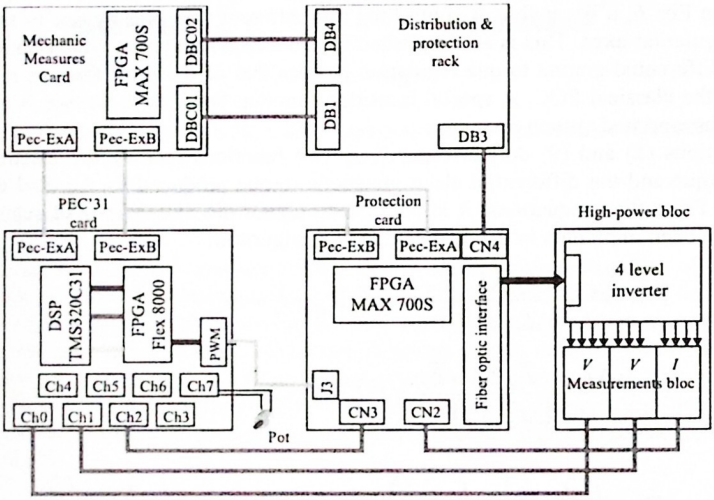

Fig. 7. Hardware for implementation of different control strategies.

5 Software Aspects

The above mentioned control structures have been implemented considering a digital-control circuit based on a DSP-FPGA association. The four digital control algorithms

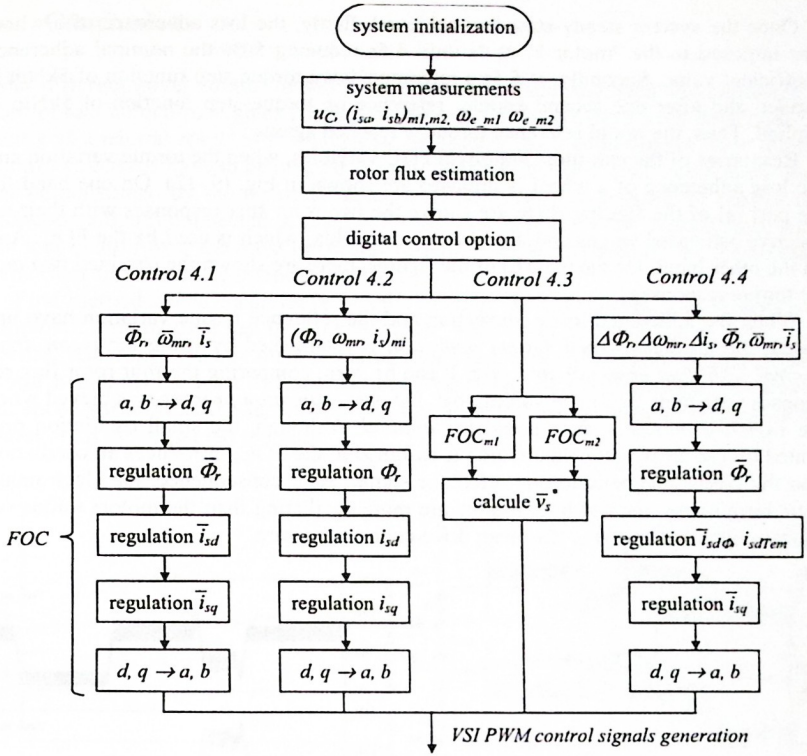

Fig. 8. Implemented algorithm control.

can be included into one main program, as it is shown in Fig. 8. An initial option will define the kind of control to be applied to the high-power system.

Our simulation study has been carried out on two main considerations. First, all modeled electrical and mechanical system components are defined either using SABER library components or created by a MAST program model. And, secondly, that the control system, which includes all the FOC proposed and the rotor flux observer algorithms, are made by a C code program. The objective of such considerations is to achieve a maximum resemblance between the global system model and the real one. The flexibility of our system model permits to incorporate all the estimated aspects in the same control component. Thus, two variables define the number of flux observers to be used and the engine drive control structure to be implemented.

Several simulations had been realized in order to analyze the system performance during imposition of external and internal perturbations. One of the most important perturbations is the loss of adherence of a wheel. Its implications for the railway traction have been explained in several works [2, 6]. Thus, in this paper, this perturbation was imposed after the system had attained the stable-state working conditions defined by: ϕ_r^*=5Wb, T_{em}^*=10kN m, and TS_{SS}^*=7m/s.

Once the system steady-state had achieved, firstly, the loss adherence of a wheel was imposed to the "motor 1" at 4s until 4.5s reducing 50% the nominal adherence coefficient value. Secondly, at 5.5s a reference down torque step function of 5kNm is applied and after one second another reference up torque step function of 5kNm is applied. Thus, the initial reference torque is reached again.

Responses of the two most important FOC variables, when the torque variation and the loss adherence of a wheel is imposed are shown in Fig. (9–12). On one hand for the part (a) of the figures, there are shown the two rotor flux responses with their respective estimated values and, the average rotor flux, which is used by the FOC. And on the other hand, for the part (b) of the figures, there are shown the obtained two motor torque responses.

When the adherence lost perturbation and the reference torque variation have imposed, the *least perturbed system operation* is established by using the *mean drive control with dual observer structure.* It can be seen, comparing the four rotor flux responses with their estimated values, that, *the best estimation process* is achieved when the *switched master - slave control is applied.* Although, the small oscillation presented by the mean rotor flux, which is assigned to the FOC, introduces an oscillation into the electromagnetic torque reference signal. As a consequence, the electromagnetic torque responses of both motors are more oscillating than the motors torque responses obtained applying the mean drive control structure.

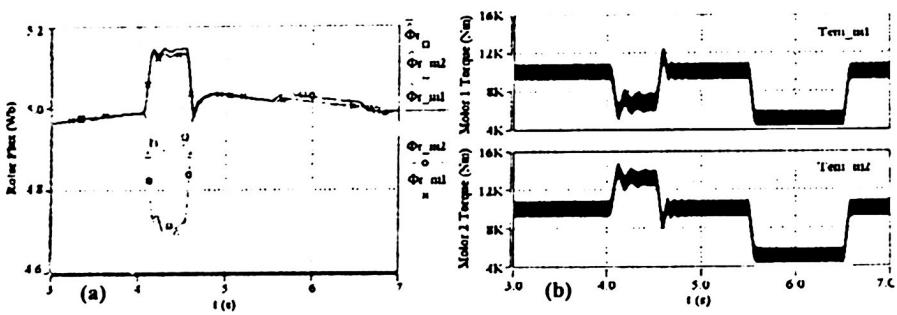

Fig. 9. The Mean Drive Control structure responses of (a) the rotor fluxes and theirs estimation values and, (b) the motor torques.

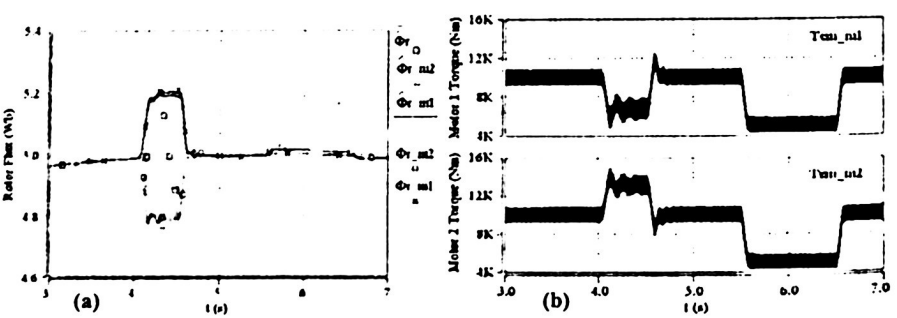

Fig. 10. The Switched Master-Slave Drive Control structure responses of (a) the rotor fluxes and theirs estimation values and, (b) the motor torques.

Once the system steady-state had achieved, firstly, the loss adherence of a wheel was imposed to the "motor 1" at 4s until 4.5s reducing 50% the nominal adherence coefficient value. Secondly, at 5.5s a reference down torque step function of 5kNm is applied and after one second another reference up torque step function of 5kNm is applied. Thus, the initial reference torque is reached again.

Responses of the two most important FOC variables, when the torque variation and the loss adherence of a wheel is imposed are shown in Fig. (9–12). On one hand for the part (a) of the figures, there are shown the two rotor flux responses with their respective estimated values and, the average rotor flux, which is used by the FOC. And on the other hand, for the part (b) of the figures, there are shown the obtained two motor torque responses.

When the adherence lost perturbation and the reference torque variation have imposed, the *least perturbed system operation* is established by using the *mean drive control with dual observer structure*. It can be seen, comparing the four rotor flux responses with their estimated values, that, *the best estimation process* is achieved when the *switched master - slave control is applied*. Although, the small oscillation presented by the mean rotor flux, which is assigned to the FOC, introduces an oscillation into the electromagnetic torque reference signal. As a consequence, the electromagnetic torque responses of both motors are more oscillating than the motors torque responses obtained applying the mean drive control structure.

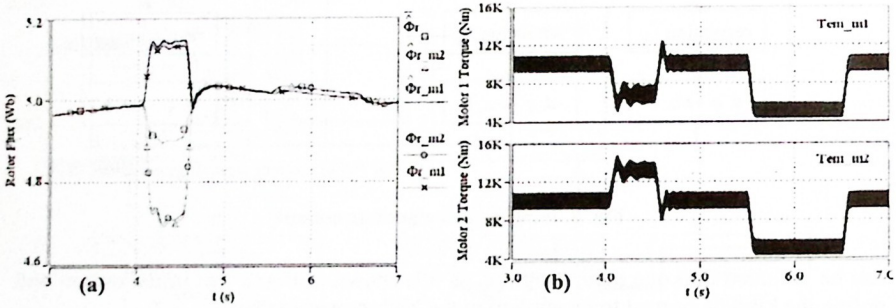

Fig. 9. The Mean Drive Control structure responses of (a) the rotor fluxes and theirs estimation values and, (b) the motor torques.

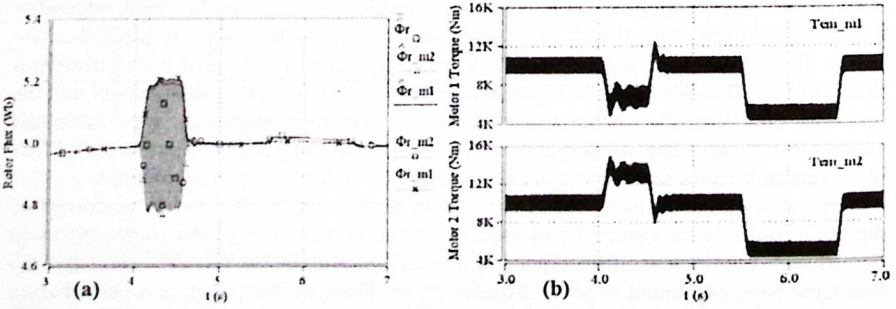

Fig. 10. The Switched Master-Slave Drive Control structure responses of (a) the rotor fluxes and theirs estimation values and, (b) the motor torques.

Switched master-slave control method presents almost the same system behavior as the first control, but the small rotor flux variation is transferred to the other system variables by the FOC algorithm. The mean drive control for dual motor is not really interesting, because its system behavior is not better than any other. In addition, its algorithm is two times longer than the first method.

Nomenclature

C_f	input filter capacitance,	v_s	stator voltage,
E	input voltage,	X	vector or matrix notation,
i_L	input filter current,	Δ	arithmetical mean difference operator, $\Delta T_{cm} = \frac{T_{cm\_m2} - T_{cm\_m1}}{2}$
IM	induction motor,		
i_{mr}	rotor magnetizing current,		
i_s	stator current,		
k_T	positive integer value,		
L_f	input filter inductance,	ϕ_r	rotor flux,
L_m	mutual inductance,	σ	leakage or coupling factor, $\sigma = 1 - L_m^2/L_rL_s$
L_s	stator self inductance,		
L_r	rotor self inductance,	τ_r	rotor time constant, $\tau_r = L_r/R_r$
P	pairs of poles number,	τ_s	stator time constant, $\tau_s = L_s/R_s$
R_f	input filter resistance,	ω	rotating reference frame frequency,
R_r	rotor resistance,		
R_s	stator resistance,	Ω	mechanical speed rotation.
T_{em}	electromagnetic torque,	ω_e	electrical speed rotation; $\omega_e = P\Omega$
T_S	sampling time period,		
TS_{SS}	steady state linear train speed,		
u_C	capacitance voltage,		

Superscripts

*	denotes a reference variable.	$\hat{}$	denotes an estimated value.
$\cdot$	denotes a time derivative.	$\bar{}$	denotes an averaged value.

Indices

$_{d,q}$	denote the axis of the rotating reference frame.
$_{\alpha,\beta}$	denote the axis of the static reference frame.
$_{1,2,3}$	denote the three-phase values.
$\_m1,\_m2$	denote a variable associated to motor 1 or to motor 2 respectively.
$\_M1,\_M4$	denote a variable associated to method control 1, ..., method control 4.

References

1. Bouscayrol, A., et al.: Multi-machine multi-converter systems: applications to electromechanical drives in EPJ Applied Physics, 10, 2, (2000) 131-147.

2. Escané, P., Lochot, Ch., Pietrzak-David, M., de Fornel, B. Electromechanical interactions in a high speed railway traction system—Comparison between two drive control structures. CD Rec. EPE 99, Lausanne, Switzerland, 7-9 September, 1999.
3. Kelecy, P. M., Lorenz, R. D. Control Methodology for Single Inverter, Parallel Connected Dual Induction Motors. IEEE PESC'94, Taipei, Taiwan, 20-25 June 1994, 2, 987-991.
4. Provoost, M., Courtois, Ch. Traction électrique ferroviaire, Dynamique ferroviaire et sous-stations. Techniques de l'Ingénieur, traité Génie électrique, D 5 501, Paris, France, (1997).
5. Peña-Eguiluz, R., Pietrzak-David, M., de Fornel, B. Observation Strategy in a Mean Control Structure for Parallel Connected Dual Induction Motors in a Railway Traction Drive System. CD Rec. EPE 2001, Graz, Austria, 27-29 August 2001.
6. Peña-Eguiluz, R., Pietrzak-David, M., Roboam, X., de Fornel, B. Dead time effect in a Railway Traction System. Proc. IEEE ISIE 2000, Puebla, Mexico, 2000, 1, 151–156.